

D.H. SHIM\*, S.S. JUNG\*\*, H.S. KIM\*\*\*, H. CHO\*\*\*, J.K. KIM\*\*\*, T.G. KIM\*\*\*, S.J. YOON\*,\*\*\*,†

## EFFECT OF CARBON NANOTUBES ON THE PROPERTIES OF SPARK PLASMA SINTERED ZrO<sub>2</sub>/CNT COMPOSITES

## WPLYW NANORUREK WĘGLOWYCH NA WŁAŚCIWOŚCI SPIEKANYCH METODĄ SPS KOMPOZYTÓW ZrO<sub>2</sub>/CNT

Zirconia matrix ZrO<sub>2</sub>/CNT composite materials reinforced with multiwall carbon nanotubes were fabricated using a spark plasma sintering technique. The effects of the amount of CNTs addition, sintering temperature and sintering pressure on the properties of the resulting ZrO<sub>2</sub>/CNT composites were examined. 0 to 9 vol. % CNTs were dispersed in zirconia powder, and the resulting mixture was sintered. The electrical conductivity, hardness, flexural strength, and density were measured to characterize the composites. The friction and wear properties of the composites were also tested. The flexural strength and friction coefficient of the composites were improved with up to 6 vol.% of CNT addition and the flexural strength showed a close relationship with the relative density of the composite. The electrical conductivity increased with increasing proportion of the CNTs, but the efficiency was reduced at more than 6 vol.% CNTs.

*Keywords:* CNT, ZrO<sub>2</sub>, Composite, SPS

### 1. Introduction

Carbon nanotubes (CNTs) [1] are excellent nanoscale fiber materials with superior mechanical [2, 3], thermal [4] and electrical [5] properties. Moreover, they can be prepared on a large scale. Therefore, CNTs have been considered as an attractive reinforcement for composite materials [6-8]. Ceramic materials exhibit superior thermal, mechanical and chemical properties compared to metals and plastics. In addition, ceramics exhibit intriguing dielectric, piezoelectric, semiconducting, and optical properties. Therefore, ceramics are used as the core materials for sensors, motors in the automotive, airplane, fuel cells, and semiconductor industries. Among the ceramic materials, zirconia ceramics have wide applications in the engineering fields because of its relatively high strength and fracture toughness. ZrO<sub>2</sub> is used widely as a refractory material in glass melt, and in iron and steel production because of its low thermal conductivity, low expansion coefficient, high chemical stability, and high strength. On the other hand, its mechanical properties, such as the fracture toughness, are still insufficient to meet the needs of many high performance ceramic parts. To overcome this, ceramic matrix nanocomposites have been developed to improve the various properties of ceramics. To fabricate these composites, spark plasma sintering (SPS) is more effective than conventional sintering because it passes an electric current with a high DC pulse voltage and simultaneously applies a high pressure. The SPS method enables the manufacture of dense materials in a short period

at low sintering temperatures compared to conventional sintering methods [9-11], and it also reduces the risk of damage to carbon nanotubes. Therefore, one way to take advantage of ceramics while compensating for these defects is to produce ceramic/CNT composites. ZrO<sub>2</sub>/CNT composites have been reported by several authors [12-16]. However, the effectiveness of CNTs on the properties of the ceramic composites is still matter of debate [15-18]. One of the reasons of this is difficulties in obtaining a homogenous distribution of CNTs throughout the matrix. A uniform dispersion of the nanotubes in the ceramic matrix is essential. Colloidal processing method [15, 19] was adopted to make the distribution of CNTs more homogenously in the matrix.

In this study, CNTs were dispersed by sonication in the zirconia powders, and followed by a wet ball-milling technique to make a uniform dispersion of CNT in the ZrO<sub>2</sub> powder. The partially stabilized zirconia matrix ZrO<sub>2</sub>/CNT composites reinforced with multiwall carbon nanotubes (MWCNTs) were fabricated using a spark plasma sintering technique. The effects of the amount of CNTs addition, sintering temperature and sintering pressure on the properties of the ZrO<sub>2</sub>/CNT composites were examined. The properties of the composites were measured and compared with each other.

### 2. Experiments

The multi-walled carbon nanotubes (MWCNT) used in this experiment were synthesized by catalytic chemical vapor

\* DEPARTMENT OF NANO FUSION TECHNOLOGY, PUSAN NATIONAL UNIVERSITY, BUSAN, 627-706, KOREA

\*\* ACNTECH, POHANG, 790-834, KOREA

\*\*\* DEPARTMENT OF NANOMECHATRONICS ENGINEERING, PUSAN NATIONAL UNIVERSITY, BUSAN, 627-706, KOREA

† Corresponding author: yoonsj@pusan.ac.kr

deposition (CCVD) with ethylene gas (C<sub>2</sub>H<sub>4</sub>) and Fe<sub>2</sub>O<sub>3</sub>-MgO as a catalyst. Partially-stabilized ZrO<sub>2</sub> powder with a mean particle size of 0.9 μ (Foskor Co., South Africa) and containing 7.38 mol. % CaO was used. 0 to 9 vol. % CNTs were dispersed by sonication in the zirconia powders, and the ZrO<sub>2</sub>/CNT composite powders were fabricated using a wet ball-milling technique for 1 hour by ACN Co. (Korea).

The composites were sintered by spark plasma sintering under vacuum conditions using a Spark Plasma Sinter (SPS-515S, Dr.Sinter Lab, Japan). The sintering temperature and applied pressure were 1150~1300° and 35~60 MPa, respectively. The on/off time of the electric pulse current was 12s/2s and the heating rate was 50°/min. The sintering temperature was maintained for 10 minutes at the target temperature. The fabricated disc type sample was 20 mmφ×7 mmH in size. Fig. 1 shows the appearance of the fabricated ZrO<sub>2</sub>/CNT composite.

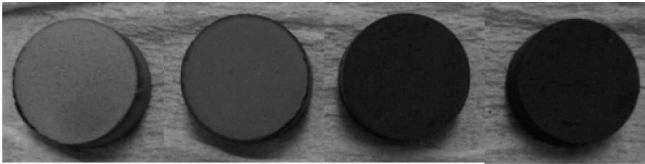


Fig. 1. Sintered ZrO<sub>2</sub>/CNTs composite specimens

The density of the fabricated composites was measured using the Archimedes method and the apparent density was calculated using Eq. (1).

$$D_a = \frac{W_1}{W_1 - W_2} \times \rho \quad (1)$$

where  $D_a$  is the apparent density,  $W_1$  is the weight of dry sample (g),  $W_2$  is the weight of sample in the liquid (g), and  $\rho$  is the specific gravity of the liquid. This value was used to calculate the relative density of the composites using Eq. (2).

$$\text{Relative density} = \frac{\text{apparent density}}{\text{theoretical density}} \times 100 \quad (2)$$

The electrical conductivity of composites was measured in air at the room temperature between -2 and 2 volts using a 2-probe type I-V measurement tester. The specimens were polished and coated with a silver paste electrode. The friction properties of the composites were tested using a ball-on-disc method without a lubricant in room temperature. The hardness and flexural strength were also measured and compared.

### 3. Results and Discussion

In Fig. 2, the relative density was shown in accordance with the CNTs content. The relative density increased when up to 3 vol. % CNTs were added but the relative density decreased with further increases in the CNT fraction. Because CNTs act as a reinforcing agent by filling up the voids of the composites, the ZrO<sub>2</sub>/CNT composites had a higher relative density than that of the monolithic ZrO<sub>2</sub>. On the other hand, sintering was interfered with the agglomeration of CNTs and tangling with ZrO<sub>2</sub> particles at higher CNT concentrations,

particularly at a CNTs fraction of 9 vol. %, consequently, the relative density decreased.

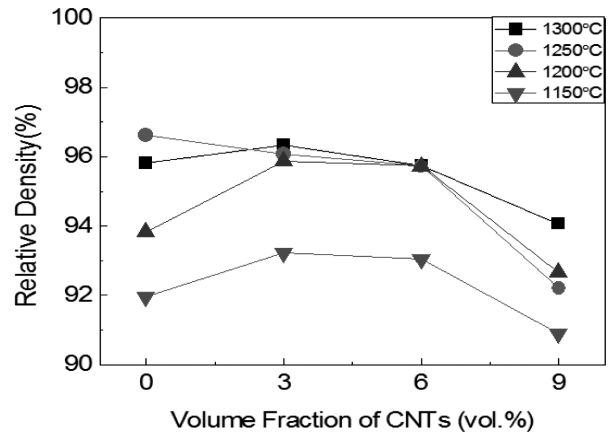


Fig. 2. Relative density of the composites as a function of the CNT content on the ZrO<sub>2</sub>/CNT composites with 60MPa by SPS

The sintering temperature has significant effects on the relative density of the composites, and the composites became more densified with increasing sintering temperature, particularly between 1150° and 1200°, and has 2~3% point increase. As the sintering temperature was increased, densification through diffusion between the particles took place more actively. The sintering pressure between 35 and 60 MPa had a marginal effect on the relative density of the composites.

Fig. 3 presents SEM images of the fracture plane that was formed by crashing the ZrO<sub>2</sub>/CNT composites spark plasma sintered at 1150° with a 60Mpa pressure. Initially, the CNTs were dispersed macroscopically among the zirconia powders, and became well conjugated, forming bonds with each other by spark plasma sintering in the ZrO<sub>2</sub>/CNT composites. As the SEM images show, significant CNT agglomeration can be observed in (c) and (d).

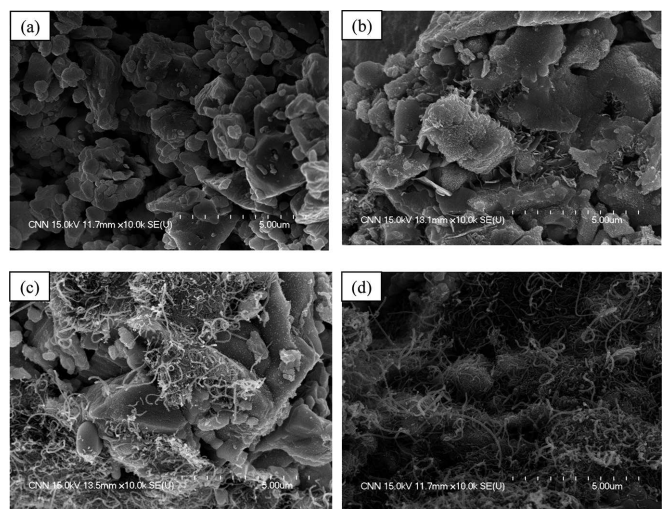


Fig. 3. SEM images of the fracture plane of the ZrO<sub>2</sub>/CNT composites sintered at 1150° with 60 MPa. (ZrO<sub>2</sub>/CNT (a) 0 vol.%, (b) 3 vol.%, (c) 6 vol.%, and (d) 9 vol.%)

Fig. 4 plots S-shaped curves of the electric conductivity of ZrO<sub>2</sub>/CNT composites versus the fraction of CNTs. The electrical conductivity increased sharply up to 6 vol. % but

sintering was not performed successfully when the proportion of CNT was increased to 9 vol. % due to agglomeration and kinking of the CNTs. Furthermore, the relative density decreased because of an increase in porosity, which serves to increase the electrical resistance. The electrical percolation phenomenon [12-15] caused by the addition of CNTs to the ceramic matrix composite, particularly in the range of 3 to 6 vol. % CNTs. Therefore, a dispersion of CNTs is important for improving this phenomenon.

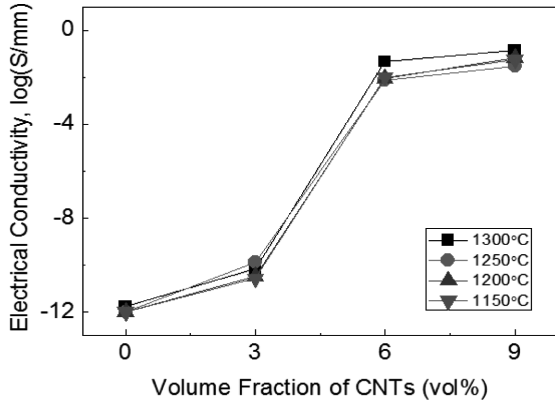


Fig. 4. Electrical conductivity of the composite materials as a function of the CNT content with 60 MPa

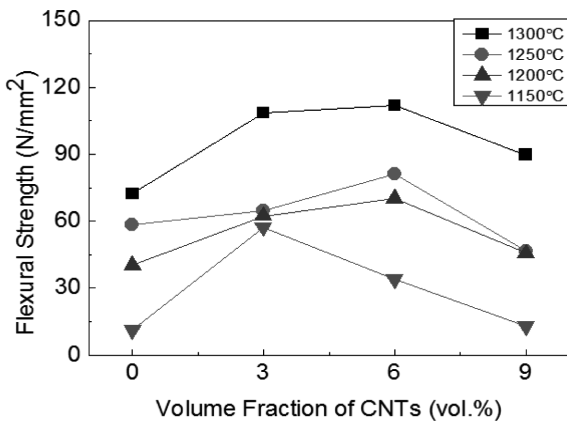


Fig. 5. Flexural strength of the composite materials at different volume fractions of CNTs with 60 MPa

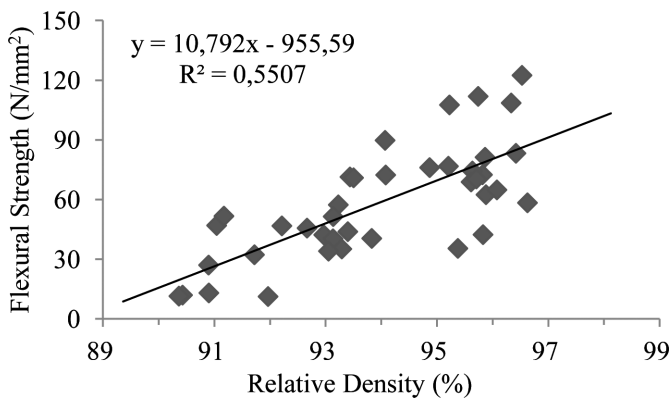


Fig. 6. Relationship between the flexural strength and the relative density of the composites

Fig. 5 shows the change in flexural strength due to the increasing CNTs content. The flexural strength increased with

increasing CNTs fraction, and the highest value above 1200° was obtained after the addition of 6 vol. % CNT. On the other hand, the flexural strength decreased with increasing CNT content. When 9 vol. % CNTs were added, the flexural strength was lower than that of monolithic TiO<sub>2</sub>. The sintering temperature also influenced the flexural strength. A close relationship exists between the flexural strength and relative density of the composite, as shown in Fig. 6. A higher relative density helps improve the strength of the composites, and this trend becomes stronger with increasing CNT content.

The fracture surface was observed to clarify the strengthening mechanism of the CNT reinforced composite, as shown in Fig. 7 (b) and (c). The CNTs connected the neighboring grains, and it appears that the composites were strengthened by grain bridging [23]. The CNTs were not only located on the surface of the particles but also penetrated into the particles, in which the interlocking particles and play the role of a bridge. The fracture surface of the monolithic TiO<sub>2</sub> shown in Fig. 7 (a) suggests that failure occurred as a result of intergranular fracture and transgranular fracture, and the microstructure of the photo shows this clearly.

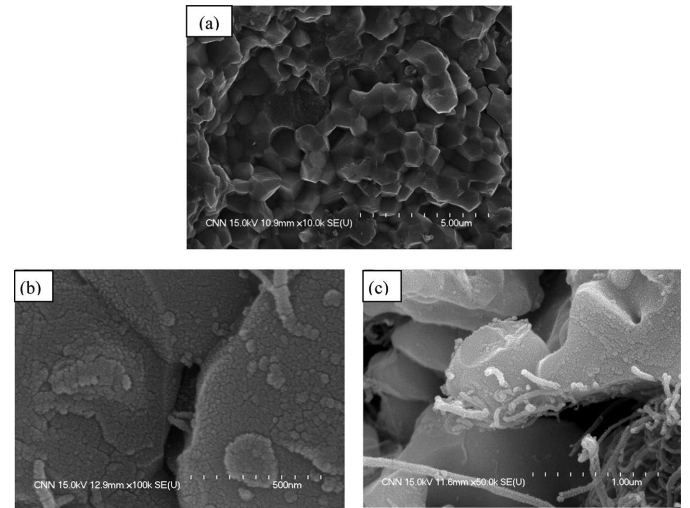


Fig. 7. SEM image of the fracture surface of (a) the monolithic TiO<sub>2</sub> and (b), (c) the ZrO<sub>2</sub>/CNT 3vol. % composite

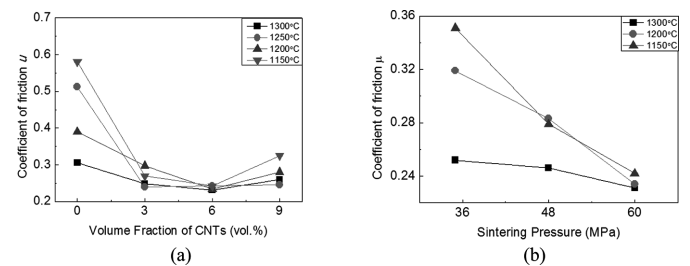


Fig. 8. Friction coefficient of the composite materials at (a) the volume fraction of CNTs with 60 MPa, and (b) the sintering pressure on the CNTs 6 vol. % addition

Fig. 8 shows the friction coefficient of the ZrO<sub>2</sub>/CNT composites. The friction coefficient decreased with increasing CNT ratio except for 9 vol. % CNT, showing a similar tendency to the flexural strength. The sintering pressure also had positive effects on the friction coefficient. Although the sintering temperature showed a significant change in the

coefficient of friction when sintered at 35 MPa, the effects were diminished compared to that sintered at 60 MPa. With CNT addition, the wear mode was converted to abrasive wear from delamination wear, and crack formation and propagation were suppressed at the grain boundary of the composites in the range of 3 to 6 vol. % CNT addition. The hardness of the composites increased with increasing CNT fraction; the hardness of the composite with 9 vol. % CNT addition was double that of the monolithic TiO<sub>2</sub>.

#### 4. Conclusions

ZrO<sub>2</sub>/CNT composites were fabricated using a spark plasma sintering technique, and the properties of the composites were examined. The relative density increased when up to 3 vol. % CNTs were added but the relative density decreased with further increases in the CNT fraction. The flexural strength and friction coefficient of the composites were improved with up to 6 vol. % of CNTs addition. The flexural strength showed a close relationship with the relative density of the composite. The wear mode was converted to abrasive wear from delamination wear with 3~6 vol. % of CNT addition. The electrical conductivity increased with increasing proportion of the CNTs, but the efficiency was reduced when 6 vol. % CNTs or more were added. Electrical percolation phenomenon was induced by CNT addition in the range of 3 to 6 vol. % of CNTs. The hardness of the composites tended to increase with increasing CNTs fraction.

#### Acknowledgements

This work was supported by a 2-Year Research Grant of Pusan National University.

#### REFERENCES

[1] S. Iijima, *Nature* **354**, 56 (1991).

- [2] M.F. Yu, O. Lourie, M.J. Dyer, K. Moloni, T.F. Kelly, R.S. Ruoff, *Science* **287**, 637 (2000).
- [3] J.P. Salvetat, A.J. Kulik, J.M. Bonard, G.A.D. Briggs, T. Stockli, K. Metenier, S. Bonnamy, F. Beguin, N.A. Burnham, L. Forro, *Adv. Mater.* **11**, 161 (1999).
- [4] J. Hone, B. Batlogg, A.T. Johnson, J.E. Fisher, *Science* **289**, 1730 (2000).
- [5] K. Kaneto, M. Tsuruta, G. Sakai, W.Y. Cho, Y. Ando, *Synth Met.* **103**, 2543 (1999).
- [6] S.J. Tans, M.H. Devoret, H. Dai, A. Thess, R.E. Smalley, L.J. Geerligs, *Nature* **386**, 474 (1997).
- [7] S. Berber, Y.K. Kwon, D. Tomanek, *Phys. Rev. Lett.* **84**, 4613 (2000).
- [8] M.J. Biercuk, M.C. Llaguno, M. Radosavljevic, J.K. Hyun, A.T. Johnson, J. E. Fischer, *Appl. Phys. Lett.* **80**, 2767 (2002).
- [9] M. Omori, *Mater. Sci. Eng.* **287**, 183 (2000).
- [10] M. Tokita, *J. Soc. Powder. Tech. Jpn.* **30**, 790 (1993).
- [11] L. Stanciu, V.Y. Kodash, J.R. Groza, *Metall. Mater. Trans.* **32**, 2633 (2001).
- [12] M. Mazaheri, D. Mari, R. Schaller, G. Bonnefont, G. Fantozzi, *Journal of the European Ceramic Society* **31**, 2691 (2011).
- [13] S.L. Shi, J. Liang, *J. Am. Ceram. Soc.* **89**, 1533 (2006).
- [14] J.P. Zhou, Q.M. Gong, K.Y. Yuan, J.J. Wu, Y.F. Chen, C.S. Li, J. Liang, *Mater. Sci. Eng. A* **520**, 153 (2009).
- [15] J. Sun, L. Gao, M. Iwasa, T. Nakayama, K. Niihara, *Ceramics International* **31**, 1131 (2005).
- [16] A. Duszová, J. Dusza, K. Tomášek, G. Blugan, J. Kuebler, *Journal of European Ceramic Society* **28**, 1023 (2008).
- [17] A. Peigney, F. Garcia, C. Estournès, A. Weibel, C. Laurent, *Carbon* **48**, 1952 (2010).
- [18] A. Datye, K. Wu, G. Gomes, V. Monroy, H. Lin, J. Vleugels, et al., *Composites Science and Technology* **70**, 2086 (2010).
- [19] N. Garmendia, I. Santacruz, R. Moreno, I. Obieta, *Journal of the European Ceramic Society* **29**, 1939 (2009).
- [20] D.J. Bergnam, *Phys. Rev. Lett.* **44**, 1285 (1980).
- [21] C.W. Nan, *Prog. Mater. Sci.* **37**, 116 (1993).
- [22] Y. Meir, *Phys. Rev. Lett.* **83**, 3506 (1999).
- [23] D.B. Marshall, A.G. Evans, *J. Am. Ceram. Soc.* **68**, 225 (1985).